IDŐJÁRÁS
Quarterly Journal of the Hungarian Meteorological Service
Vol. 114, No. 4, October–December 2010, pp. 251–261

Analysis of climate change in Hungary according to an extended Köppen classification system, 1971–2060

Áron Péter Fábián[1] and **István Matyasovszky**[2]

Department of Meteorology, Eötvös Loránd University,
P.O. Box 32, H-1518 Budapest, Hungary
E-mails: [1]csigaa@gmail.com, [2]matya@ludens.elte.hu

(Manuscript received in final form August 31, 2010)

Abstract—The purpose of this paper is to provide information on tendencies of the climate change in the area of Hungary (48.3°–45.5° W; 16.0°–22.3° E) between 1971 and 2060. Future climate change results obtained from climate models are not used directly due to their uncertainties and inaccuracies, but spatio-temporal distribution of climate classes of the Köppen climate classification system is analyzed. It has become clear that the Köppen system is unable to indicate the expected warming of the summer in certain cases, thus, two additional climate classes are introduced. Two datasets are used, the CRU TS 1.2 (with a spatial resolution of $1/6 \times 1/6$ degrees) for observed temperature and precipitation, and TYN SC 1.0 (same resolution) for climate model generated data. In the latter case, all the four available emission scenarios (A1FI, A2, B1, B2) are analyzed. The climate class of each grid box is calculated for each year from temperature and precipitation data, then the changes of areas covered by the classes resulted from the previous step are analyzed. The evaluation of tendencies is based on 10- and 30-year climate average maps and on the extremes of yearly values of each class. It is found that climate extremes will strengthen in the future during a nearly constant warming. Additionally, the more and more frequent appearance of the steppe climate and the constant presence of the dry-summered class at the end of the period show growing aridity in the area.

Key-words: climate change, climate model, Köppen climate system, warming, drought

1. Introduction

Assessment of both the climate change experienced in recent decades and regional characterization of the anticipated global climate change is in the focus of research. The purpose of this paper is to provide information on tendencies of the climate change in the area of Hungary between 1971 and 2060. As the global or even regional climate models reproduce the observed climate with high inaccuracies (*Bartholy et al.*, 2006; *Bartholy et al.*, 2008; *Szépszó* and *Horányi*, 2008) over the area of Hungary, future climate change results obtained from these models are not used directly but spatio-temporal distribution of climate classes of the Köppen climate classification system is analyzed.

Because model generated values of meteorological variables are used to determine these climate classes, their inaccuracies might result in climate class uncertainties. However, the applied classification methods are quite insensitive to deviations and errors (*Beck et al.*, 2006).

2. Data and methods

2.1. The Köppen climate classification system

The Köppen climate classification system is a so-called effective system. It classifies the climate by environmental characteristics and given threshold values of given climate components. The components used for classification are: annual mean temperature (t), annual precipitation amount (r), monthly average temperatures of the summer and winter months, monthly precipitation amounts of the summer and winter months, mean temperature of the summer and winter, precipitation amounts of the summer and winter, monthly mean temperatures of the 4 warmest months, monthly mean temperature of the coldest month, and elevation above the sea level. Threshold values of the climate classes which are likely to appear in Hungary are described in *Tables 1–3* according to *Critchfield* (1983).

Table 1. Arid Köppen climate classes according to *Critchfield* (1983)

Class	**Description**	**Precipitation limit *r* (cm)**	**Temperature limit *t* (°C)**
Arid with winter precipitation: at least 70% of the annual precipitation falls in the 6 coldest months, and $r < 2t$ applies			
BW	Desert	$r < t$	-
BSh	Warm steppe	$r > t$	$t > 18$
BSk	Cold steppe	$r > t$	$t < 18$
Arid with summer precipitation: at least 70% of the annual precipitation falls in the 6 warmest months, and $r < 2(t + 14)$ applies			
BW	Desert	$r < t + 14$	-
BSh	Warm steppe	$r > t + 14$	$t > 18$
BSk	Cold steppe	$r > t + 14$	$t < 18$
Arid with balanced precipitation: less than 70% of the annual precipitation falls in either halves of the year, and $r < 2(t + 7)$ applies			
BW	Desert	$r < t + 7$	-
BSh	Warm steppe	$r > t + 7$	$t > 18$
BSk	Cold steppe	$r > t + 7$	$t < 18$

Table 2. Temperate rain Köppen climate classes according to *Critchfield* (1983)

Class	Description	Summer (warmest month)	Winter (coldest month)	Precipitation
Cs	Arid in summer	Mean temperature over 10 °C	Mean temperature over -3 °C	Sum of the most arid summer month is less than 4 cm, and also less than the tierce of the precipitation sum of the most humid winter month
Cw	Arid in winter	Mean temperature over 10 °C	Mean temperature over -3 °C	Sum of the most arid winter month does not exceed the tenth of the precipitation sum of the most humid summer month
Cfa	Balanced precipitation	Mean temperature over 22 °C	Mean temperature over -3 °C	Balanced
Cfb	Balanced precipitation	Mean temperature over 10 °C for 4 months	Mean temperature over -3 °C	Balanced
Cfc	Balanced precipitation	Mean temperature over 10 °C	Mean temperature over -3 °C	Balanced

Table 3. Boreal forest and snow Köppen climate classes according to *Critchfield* (1983)

Class	Description	Summer (warmest month)	Winter (coldest month)	Precipitation
Ds	Arid in summer	Mean temperature over 10 °C	Mean temperature below -3 °C	Sum of the most arid summer month is less than 4 cm, and also less than the tierce of the precipitation sum of the most humid winter month
Dw	Arid in winter	Mean temperature over 10 °C	Mean temperature below -3 °C	Sum of the most arid winter month does not exceed the tenth of the precipitation sum of the most humid summer month
Dfa	Balanced precipitation	Mean temperature over 22 °C	Mean temperature below -3 °C	Balanced
Dfb	Balanced precipitation	Mean temperature over 10 °C for 4 months	Mean temperature below -3 °C	Balanced
Dfc	Balanced precipitation	Mean temperature over 10 °C	Mean temperature below -3 °C	Balanced
Dfd	Balanced precipitation	-	Mean temperature below -38 °C	Balanced

The original classification system is inappropriate to represent warming trends in such environments where the thresholds of Cfa or Dfa apply, but the highest monthly mean temperature is far above 22 °C. There is a need, therefore, to introduce additional climate classes to identify the warming of the climate regions with already hot summer in the beginning of the time series. Of course, the original methodology of the system is kept in sight. The newly-introduced classes are:

– **Cfa+**: the monthly mean temperature exceeds 22 °C for at least 4 months,
– **Dfa+**: the monthly mean temperature exceeds 22 °C for at least 4 months.

2.2. The CRU TS 1.2 data set

The *CRU TS 1.2* (*Mitchell et al.*, 2004) is a gridded data set of monthly means and sums of several climate variables for the period of 1901–2000 with a resolution of $1/6 \times 1/6$ degrees. Its spatial coverage is defined by the 11° W–32° E longitudes and 34°–72° N latitudes including the entire continent of Europe. Actually, temperature means and precipitation totals are used over an area with latitudes 48.3°–45.5° N and longitudes 16.0°–22.3° E represented by $18 \times 40 = 720$ grid boxes.

2.3. The TYN SC 1.0 data set

The *TYN SC 1.0* (*Mitchell et al.*, 2004) is a gridded data set of monthly means and sums of several climate variables for the period of 2001–2100 with a spatial coverage and resolution as in the case of the CRU TS 1.2 data set. It does not contain raw model output, but its values are derived from the means of 1961–1990, the variability of 1961–1990, and a model provided response pattern to the rise of temperature. This method, although does not use downscaling of the model-generated data, can give more accurate results than raw model output as it bypasses the inaccurate prediction process of mean and variability, and replaces them by real observed data (*Mitchell et al.*, 2004).

Temperature means and precipitation amounts obtained from the HadCM3 (*Gordon et al.*, 2000) climate model with 4 scenarios (A1FI, A2, B1, B2) (*IPCC*, 2000) are used. The A1FI scenario expects a future with fast technological development and convergence between regions, but strong reliance on fossil fuels. The A2 describes a more heterogeneous, less technically developed world. The B1, like A1, assumes convergence, but along with changes in economical structure and more usage of resource-effective technologies. The B2 works with slower, more locally focused development, but also optimal environmental politics, unlike A2.

2.4. Software used for data processing

Calculations have been performed with an own developed software written in the Python programming language. A scheme of its operation is shown in *Fig. 1*, a more detailed discussion can be found in the Appendix. Three kinds of products were made: climate maps for each analyzed periods (10-year average maps from the observed and 30-year average maps from the predicted datasets), extremes plots showing the minimum and maximum gridbox numbers covered by all climate classes in all years of the analyzed period, and annual spatial mean temperature diagrams for each analyzed period.

The analysis of climate change was mainly based on the average maps; the extreme plots were used to indicate the variability during the analyzed periods. For instance, an arid climate class with relatively high maximum value indicates that although this class may not appear on the average map (wetter years compensate it), there were droughts during the analyzed period.

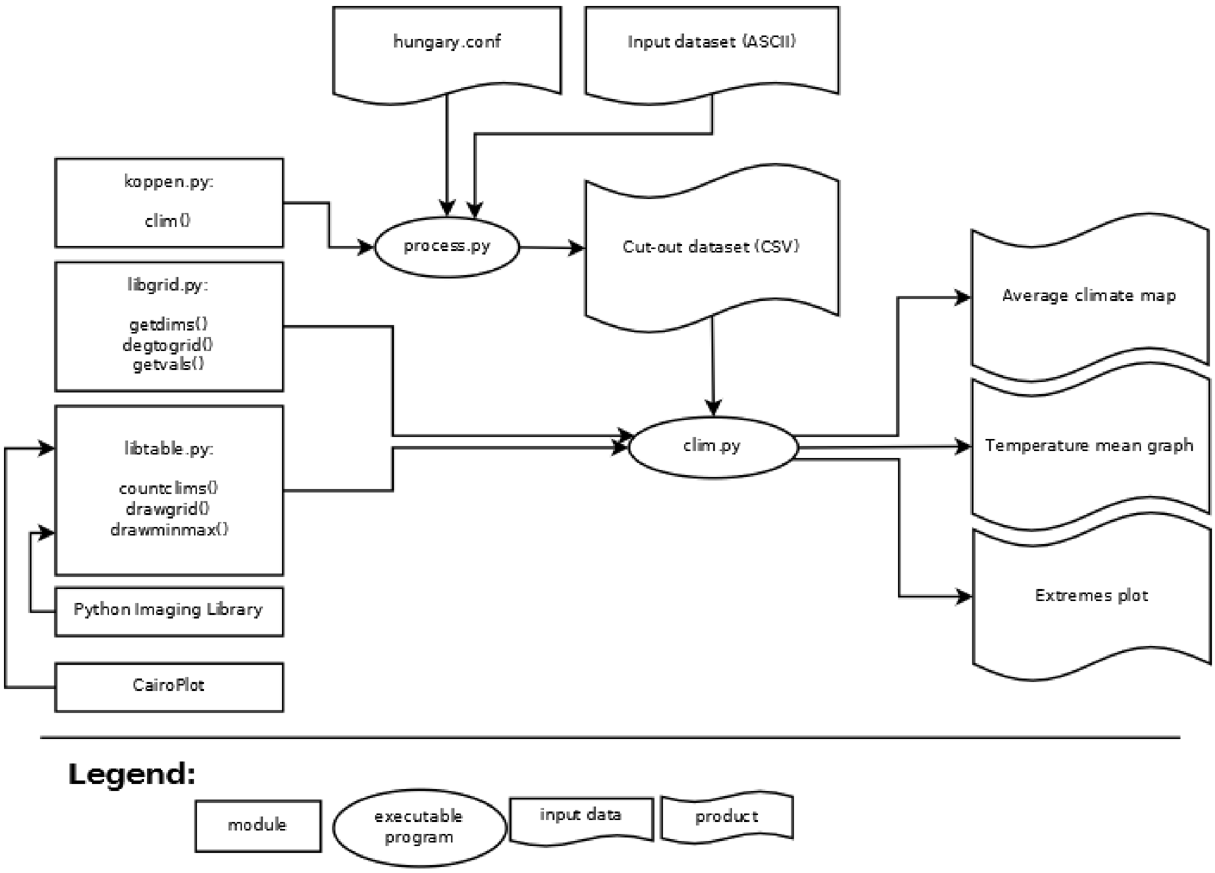

Fig. 1. A scheme of the software used for Köppen climate classification.

3. Results

3.1. Observed data

The climate of Hungary, according to the averages of the period 1951–2000 is classified as mild wintered and moderately warm summered Cfb class (*Kottek et al.*, 2006). However, the analysis of the years from 1971 to 2000 with the above mentioned higher spatial resolution produces more precise and quite different results. The time series of annual spatial mean temperatures (*Fig. 2*) shows a quasi-constant rise with minor declines that can also be observed in the occupied areas of the climate classes through the period.

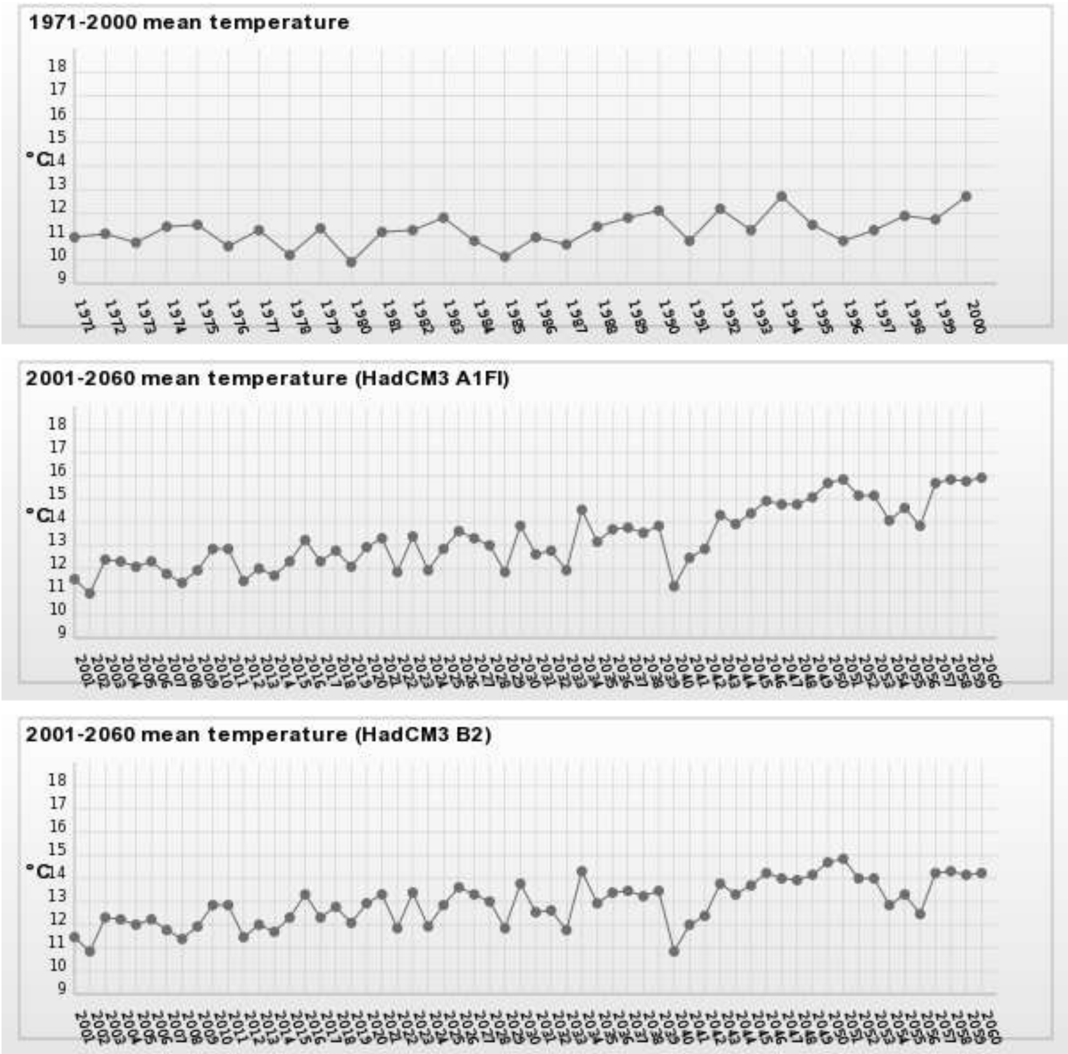

Fig. 2. Spatially averaged annual mean temperature for the periods of 1971–2000 (top) and 2001–2060 for scenarios A1FI (middle) and B2 (bottom).

3.1.1. The 1970s (1971–1980)

The climate average map of the 1970s (*Fig. 3*) shows an almost concentric spatial distribution: the middle of the basin is dominated by the hot summered and mild wintered Cfa, the hill and mountain regions are covered by the cooler summered Cfb, while the north is accompanied by the colder wintered Dfb. The extremes plot shows remarkable Cw-Cs and Cfb-Dfb fluctuations. The prior indicates intense oscillations in the distribution of precipitation through the years; the latter shows the same in mean temperature of the winter.

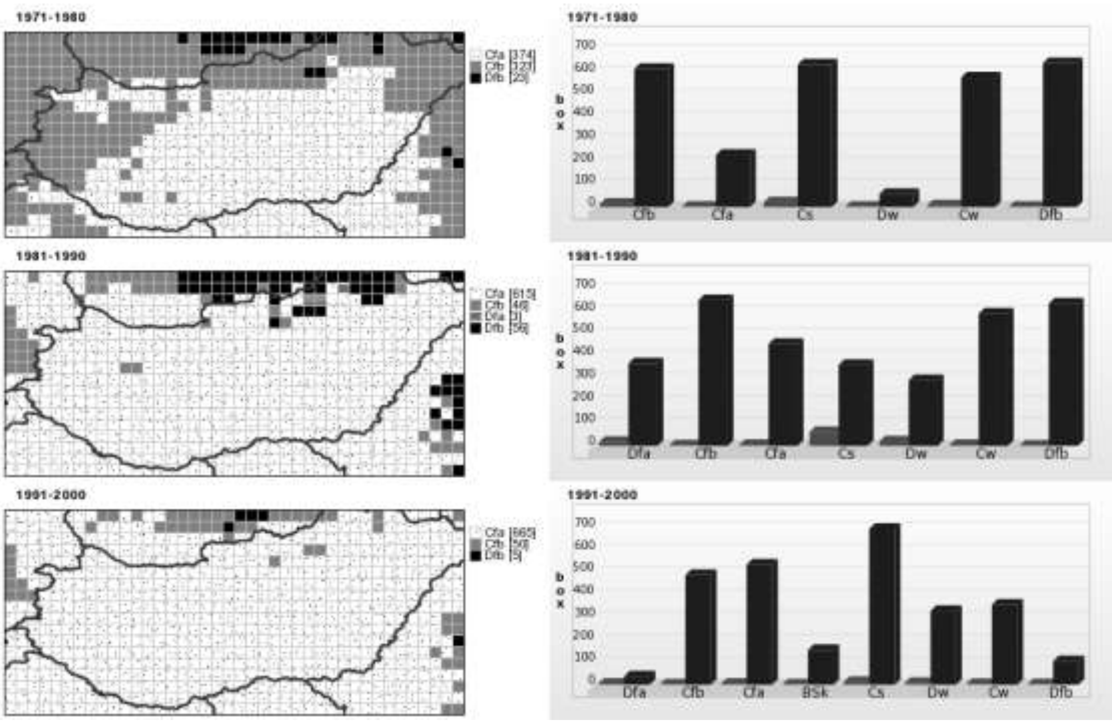

Fig. 3. Spatial distribution of Köppen climate classes with numbers of grid boxes (in parentheses) corresponding to different classes (left), and maximum (dark) and minimum (bright) numbers of grid boxes corresponding to different climate classes in individual years of the ten-year periods of 1971–2000 (right).

3.1.2. The 1980s (1981–1990)

On the average map of the 1980s (*Fig. 3*), the area of Cfa grows remarkably on the expense of Cfb (warming of summer), and the border of the northern Dfa zone expands to south suggesting the cooling of winters in these territories. The extremes plot shows again the Cfb-Dfb fluctuation started in the previous decade, but with lesser disturbances of the annual temporal distribution of precipitation (reduction of Cs area) and with somewhat major fluctuations in the mean temperature (Cw-Dw – mild or cold winter) as compared to the 1970s. These changes show a cooling in this decade identified also in the 30-year spatial mean temperature plot. The lower summer mean temperatures explain the phenomenon (*Szalai et al.,* 2005).

3.1.3. The 1990s (1991–2000)

In the 1990s (*Fig. 3*), the expansion of the Cfa area and the narrowing of colder climates continues. After the temporary decline during the previous decade, the rise of mean temperature returns. This tendency can also be observed in the extremes plot where the D classes are almost missing. Additionally, the considerably high maximum of the dry-summered Cs class with appearance of the steppe (BSk) show rising aridity with general and summer-specific precipitation reduction in the area.

3.2. Climate model generated data

The period 2001–2060 was analyzed according to the four emission scenarios. The scenarios generated similarly fluctuating spatial mean temperature curves (*Fig. 2*), but the slopes differ in each scenario. The entire period was divided into two intervals including the years 2001–2030 and 2031–2060, respectively. All scenarios produced similar results for the near-future period (2001–2030), so only one scenario (A1FI) is presented in this case. However, two scenarios – one with the least extreme changes (B2) and one with the most extreme changes (A1FI) – are presented for the latter period (2031–2060).

3.2.1. The period 2001–2030

The climate average map of this period is similar to the previous one (1990s) but with more Cfb in the borders of the basin indicating colder summers in these areas (*Fig. 4*). Additionally, the Dfb almost vanishes in this area showing the warming of the winters. In the middle of the basin, the mild-wintered, hot-summered Cfa still dominates. The extremes diagram is also very similar to the 1990s. The Cw and BSk maximums are higher on the expense of Cs, so the rise of aridity continues throughout this period.

3.2.2. The period 2031–2060 (A1FI)

The most intense climate change was obtained with scenario A1FI in this period (*Fig. 4*). On the average map, the Dfb fully and the Cfb almost vanishes. In the southern region, a big area of the very hot summered Cfa+ emerges. These changes unanimously indicate the warming of the summer. The majority of the basin remains Cfa. On the extremes plot, the maximum levels of BSk and Cs are remarkably higher than in the previous period, so very dry years can be counted on. As the Cw reduces the precipitation distribution has changed throughout the year. The relatively high maximum and minimum of Dfa+ (cold winter, very hot summer) shows extreme fluctuations of the temperature throughout the year in some regions.

3.2.3. The period 2031–2060 (B2)

The B1 scenario shows more similar picture to the previous period (*Fig. 4*). On the average climate map, the Cfb area reduces remarkably, although some Dfb remains. The coverage of Cfa+ in the south is also smaller. These effects involve a more moderate warming compared to A1FI. The extremes plot also shows milder changes: the maximum of BSk reduces, but the rising of Cs (observed in A1FI) is also unharmed here. The reduction of Cw is also observable, but the Dfa+ is weaker as compared to A1FI. To summarize, the B2 scenario shows almost the same changes as A1FI, but with a remarkably smaller level.

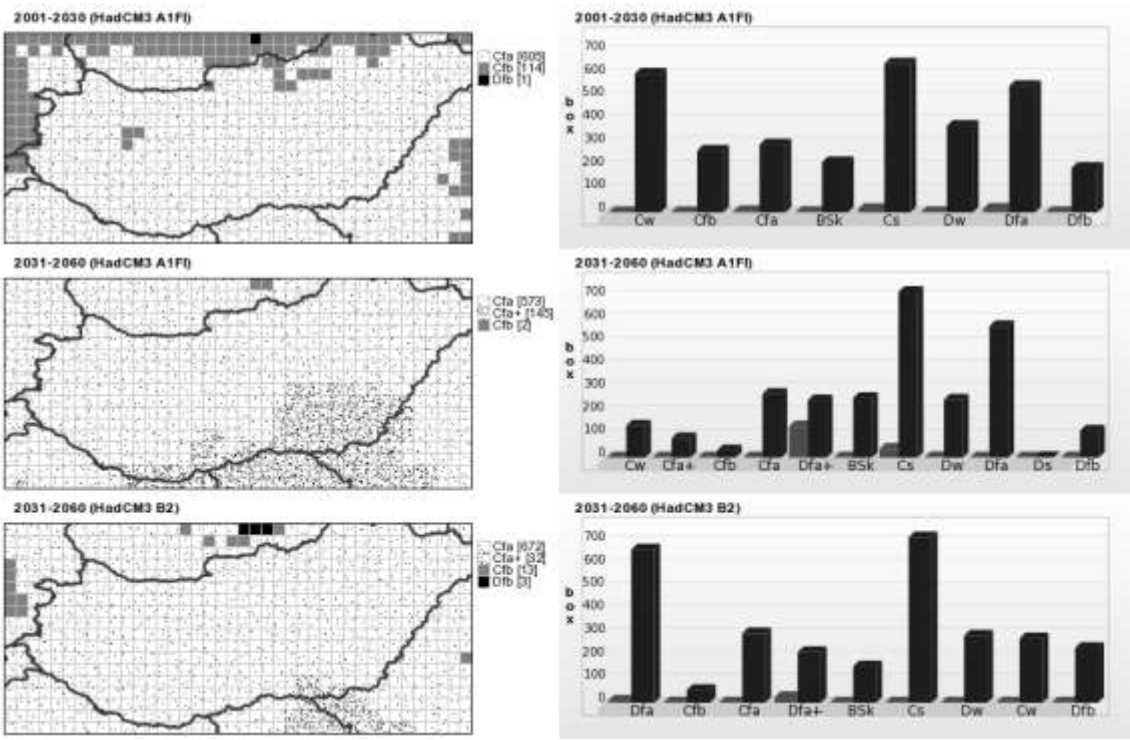

Fig. 4. Spatial distribution of Köppen climate classes with numbers of grid boxes (in parentheses) corresponding to different classes (left), and maximum (dark) and minimum (bright) numbers of grid boxes corresponding to different climate classes in individual years of the thirty-year periods of 2001–2060 (right).

4. Conclusions

The dominant climate class of the observed period 1971–2000 was Cfa in contrary to *Beck*'s (2006) results. Although the yearly results showed fluctuations with different magnitudes of the mean temperature and precipitation distribution, the area of Cfa extended on expense of the colder wintered and summered climate classes. This tendency fully coincides with the almost constant rise of mean temperatures observed in the period. Additionally, the emergence of steppe (BSk) in the last decade means minor drying.

In the climate model generated datasets, a warming tendency evidently exists. Also, the summer precipitation unanimously reduces in some years (see the high Cs maxima) and the occurrences of steppe (BSk) are also unharmed, so occasional droughts can be counted on. The different scenarios show these same changes but with different magnitudes, the most extreme is A1FI, and the least is B2. In A1FI, the strong presence of the Dfa+ (a class with cold winter and very hot summer) predicts extreme fluctuations of temperature in some years of the period.

The above discussed qualitative results coincide with the conclusions of IPCC for the future climate of Europe (*Alcamo et al.*, 2007). As the Köppen classification system is based on vegetation groups (*Peel et al.*, 2007), the results of this study can be used for various environmental, climatological, and agricultural purposes.

Also, a survey suggested that maps illustrating projected shifts of Köppen climatic zones are an effective visualization tool for disseminating climate change information (*Jylhä et al.*, 2010). Previous similar studies working on global (*Rubel* and *Kottek*, 2010) or continental (*Jylhä et al.*, 2010) scales give climate change information on relatively coarse spatial resolutions. For instance, an analysis of *Jylhä et al.* (2010) for Europe shows major future climate changes in the Iberian Peninsula, around the Black Sea and in the Alps. They found the regions with temperate (Cf, Cs) and dry climates (BW, BS) expanding. However, the entire area of Hungary is assigned here to Cfb class using data of the last five decades, and the projected future shifts of Köppen climatic zones are roughly represented as compared to our fine resolution approach. Also, presentation of extreme appearance of the different climate classes within the periods examined is an added product.

Since model generated values of meteorological variables are used to determine the climate classes, model output inaccuracies might result in climate class uncertainties. However, the applied classification methods are quite insensitive to deviations and errors (*Beck et al.*, 2006); see the threshold widths of the climate classes. Also, the raw model output is adjusted in the TYN 1.0 data set with a procedure reproducing much better the observed climate, and this procedure is then applied to model outputs corresponding to the future climate. This adjustment is expected to deliver more reliable model generated data (*Mitchell et al.*, 2004).

References

Alcamo, J., Moreno, J.M., Nováky, B., Bindi, M., Corobov, R., Devoy, R.J.N., Giannakopoulos, C., Martin, E., Olesen, J.E., and *Shvidenko, A.*, 2007: In *Climate Change 2007: Impacts, Adaptation and Vulnerability.* Contribution of Working Group II to the Fourth Assessment Report of the Intergovernmental Panel on Climate Change, Cambridge University Press, UK, 541-580.

Bartholy, J., Pongrácz, R., Torma, Cs., and *Hunyady, A*, 2006: *Modelling Regional Climates and Adapting the PRECIS Climate Model* (in Hungarian). Országos Meteorológiai Szolgálat, Budapest, pp. 228.

Bartholy, J., Pongrácz, R., Gelybó, Gy., and *Szabó, P.*, 2008: Analysis of expected climate change in the Carpathian Basin using the PRUDENCE results. *Időjárás 112,* 249-264.

Beck, C., Grieser, J., Kottek, M., Rubel, F., and *Rudolf, B.*, 2006: Characterizing global climate change by means of Köppen climate classification. *Klimastatusbericht KSB* 2005, 139-149.

Critchfield, H. J., 1983: *General Climatology*. 4th ed. Prentice Hall, 453 pp.

Gordon, C., Cooper, C., Senior, C.A., Banks, H., Gregory, J.M., Johns, T.C., Mitchell, J.F.B., and *Wood, R.A.*, 2000: The simulation of SST, sea ice extents and ocean heat transports in a version of the Hadley Centre coupled model without flux adjustments. *Clim. Dynam. 16,* 147-168.

IPCC, 2000: *Special Report on Emission Scenarios*. Cambridge University Press, UK, 570 pp.

Jylhä, K., Tuomenvirta, H., Ruosteenoja, K., Niemi-Hugaerts, H., Keisu, K., and *Karhu, J.A.*, 2010: Observed and projected future shifts of climatic zones in Europe, and their use to visualize climate change information. *Wea. Climate Soc. 2,* 148-167.

Kottek, M., Grieser, J., Beck, C., Rudolf, B., and *Rubel, F.*, 2006: World Map of Köppen-Geiger Classification Updated. *Meteorol. Z. 15,* 1-5.

Mitchell, T.D., Carter, T.R., Jones, P.D., Hulme, M., and *New, M.*, 2004: A comprehensive set of high-resolution grids of monthly climate for Europe and the globe: the observed record (1901–2000) and 16 scenarios (2001–2100). *Tyndall Centre Working Paper No. 55.*, URL: *http://www.ipcc-data.org/docs/tyndall_working_papers_wp55.pdf.*

Peel, M.C., Finlayson, B.L., and *McMahon, T.A.,* 2007: Updated world map of the Köppen-Geiger climate classification. *Hydrol. Earth Syst. Sci. Discuss. 4,* 439–473.

Rubel, F. and *Kottek, M*., 2010: Observed and projected shifts 1901–2100 depicted by world maps of Köppen-Geiger climate classification. *Meteorol. Z. 19,* 135-141.

Szalai, S., Konkolyné Bihari, Z., Lakatos, M., and *Szentimrey, T.*, 2005: *Some Characteristics of the Climate of Hungary from 1901* (in Hungarian). Országos Meteorológiai Szolgálat, Budapest.

Szépszó, G. and *Horányi, A.*, 2008: Transient simulation of the REMO regional climate model and its evaluation over Hungary. *Időjárás 112*, 203-231.

Appendix

The software group used for data processing consists of three common libraries (the koppen module for climate classification, the libgrid module for database processing, and the libtable module for producing climate maps and charts), a process program creating a sub-area including Hungary from the full dataset, and the clim program used to perform the analyses.

The koppen module's only function is clim(). This function is used to classify the climate of a year according to the Köppen system based on the given monthly mean temperatures and monthly precipitation totals, hemisphere (determining which months belong to winter and summer) and elevation data.

The functions of the libgrid module are the getdims() that reads the needed information from the headers of the data files, the degtogrid() that converts degree values to grid coordinates, and the getvals() that extracts the time series of the given grid boxes for the given dates.

The libtable module consists of countclims() creating the occurrence frequencies of the climates in a table, drawgrid() drawing a grid map using the values of the table, drawminmax() plotting the maximal and non-zero minimal area coverage data of all the climate classes in a given dataset. The Python Imaging Library and the CairoPlot module were used for drawing and plotting, respectively.

The process program creates a cut-out from the dataset according to the given geographical and temporal coordinates recorded in the configuration file hungary.conf, classifies the climates of all grid boxes in the cut-out, and saves them into a CSV data table. The difference between the process programs used for analyzing the observed and model generated datasets is that the program for the model data sets needs the name of the emission scenario (A1FI, A2, B1, B2) in command line argument; in addition, it indicates the scenario in the output file names.

The clim program uses the output files of the process. It draws the decadal mean climate maps, the spatial mean temperature graphs for the entire period, and the bar plots with the functions of the libtable. The program for the model generated datasets also needs the name of the emission scenario (A1FI, A2, B1, B2) in command line argument.

These programs are not actually available for public use, but development of their user friendly version is in progress.